

Design and Optimization of Conformal Dielectric Resonator Antenna Array Based on Aperture-Coupled Series-Feeding Approach

Hongmei Liu*, Yue Niu, Tielin Zhang, Shaojun Fang, and Zhongbao Wang

Abstract—A novel conformal dielectric resonator antenna (DRA) array based on aperture-coupled series-feeding approach is presented for wireless communication. The antenna is composed of eight curved width-gradated DRA elements with a simple feeding structure. The proposed design presents a tapered current amplitude distribution by using DRA element width gradation method, and low side-lobe level (SLL) characteristic can be obtained. Besides, an extra matching line is inserted into the single feeding line to realize better impedance characteristic. To validate the performance of the proposed design, the conformal array is fabricated and measured in an anechoic chamber. The measured impedance bandwidth ($|S_{11}| < -10$ dB) of the fabricated prototype is from 5.78 GHz to 5.87 GHz. At 5.8 GHz, the antenna offers a measured peak gain of 14.75 dBi and SLL of -19.3 dB. The polarization discriminations of the array on E - and H -planes are greater than 20 dB. The measured results of the fabricated prototype demonstrate that the proposed design has the potential to be applied to wireless communication system with curved surface.

1. INTRODUCTION

Dielectric resonator antenna (DRA) can be considered as a successful candidate for wireless communication, especially in the microwave and millimeter frequency bands, owing to its inherent advantages of compact size, high power handling capability, low conduction losses, and high radiation efficiency [1–3]. In general, feeding methods including probe, microstrip line, coplanar waveguide, and aperture-coupled are applied to excite the DRA efficiently [4–7]. Among them, aperture-coupled feeding technology is more preferred since an extra resonance is introduced by the coupling slot, and wide impedance bandwidth can be easily obtained. Besides, owing to the electric wall effect of the ground plane, the E -field distribution of the DR elements can be mirrored, so the actual height of the antenna can be halved with no degradation of its pattern [4].

Recently, to fulfil the demand for high gain antenna, high-gain DRA arrays have been widely studied [8–14]. In [8], a high-gain DRA array fed by a radial-line waveguide is presented. Although the measured gain is 26.7 dBi, the bandwidth is narrow (1%). In [9], the DRA array based on novel standing-wave feeding approach is introduced. The measured peak gain is about 15 dBi with the relative bandwidth of 7%. The only disadvantage is that the antenna covers a large area with a high profile. To reduce the profile, a dielectric patch resonator with silver-coated slots is presented, and a 1×4 array is designed [10]. The measured impedance bandwidth is about 17%, and the peak gain is 13.55 dBi. However, the complex manufacturing process and high cost limit its application. In [11], a ten-element perforated rectangular DRA array is designed. The measured peak gain can reach 15.7 dBi with an impedance bandwidth of 36.1%. However, since the air gap between the double-layer dielectric substrates is difficult to control, the measurement errors can be caused easily. In [12] and [13], SIW-fed DRA arrays are presented. However, due to SIW feeding technique, the bandwidths are narrow

Received 27 November 2020, Accepted 20 January 2021, Scheduled 26 January 2021

* Corresponding author: Hongmei Liu (lhm323@dlmu.edu.cn).

The authors are with the School of Information Science and Technology, Dalian Maritime University, Dalian, Liaoning 116026, China.

(< 9%), and the SLLs are unsatisfied (about -10 dB). Large size is also exhibited. In [14], a low side-lobe level (-23.01 dB) and wideband (38.1%) linear DRA array is presented with series-feeding technique. However, since the Chebyshev amplitude distribution is achieved by tuning the impedance of each feeding line, the design is complicated. Moreover, due to the use of slot windows, a reflector has to be added for unidirectional radiation, resulting in large size. Except the DRA antenna array, multi-layer structures and reflectors are also efficient for gain enhancement. In [15], four superstrate layers and a reflector layer are used to obtain a significant gain increase of 4.3 dB. Besides, the SLL of radiation pattern is reduced, and a front-to-back ratio of 18.55 dB is achieved with the aid of the reflector. In [16], a high-gain circularly polarized antenna array is proposed. By using the metal reflector, the gain reaches 9.33 dBic.

Most of the reported high-gain antenna arrays are concentrated on planar arrays. Except planar arrays, conformal arrays, due to their unparalleled advantages of reduced aerodynamic drag, high space utilization, and wide-angle coverage, have received more and more attention in modern communication systems [17]. Among conformal arrays, cylindrically conformal antenna is more preferred [18–21] after considering the simple processing and low influence of the bending substrate on radiation performance. In [18], a cylindrically conformal slot array fed by a 1 to 4 microstrip feed network is proposed to obtain an enhanced axial radiation. The impedance bandwidth is 12.5%, but its measured peak gain of axial radiation is only 5.12 dBic. In [19], a circumferentially conformal array fed by SIW is presented. The measured peak gain is about 11 dBi, but the impedance bandwidth is narrow (< 2%). In [20], a wideband cylindrically conformal phased array antenna is presented. It achieves 3 : 1 impedance bandwidth with a realized gain of above 10 dBi, but the complex structure and fabrication process limit its actual applications. In [21], a conformal series-fed comb-line microstrip array design is presented. It owns simple structure and low profile, but its maximum gain is only 10 dBi, and the impedance bandwidth is narrow (3%). To date, no conformal DRA array is reported with a simple structure and good performance.

In this paper, a conformal DRA array with high gain and low SLL is presented. It is composed of eight bent rectangle DR elements, eight conformal rectangle slots, and one conformal feeding line. Since the field distribution is sparser and the quality factor is lower for the convex bent DRA than a rectangle DRA, broader bandwidth can be obtained. To simplify the structure, a conformal single microstrip feeding line combined with conformal slots is used for exciting the array antennas. To realize low SLL, the widths of the bent DRAs are adjusted to obtain suitable current amplitude distribution. An extra matching line is also inserted into the feeding line to obtain better impedance characteristic. Finally, a prototype has been fabricated and measured with the aid of an anechoic chamber to demonstrate the excellent radiation characteristic of the proposed design.

2. APERTURE-COUPLED SERIES-FEEDING DRA ARRAY

The geometry of the conformal array is shown in Figure 1. It is composed of eight conformal DRA elements, which are placed on the slots loaded ground plane of the conformal substrate. To maximize the coupling energy fed to the DRAs, eight parallel slots are located below the middle of each DRA element. On the other side of the substrate, a conformal feeding line is etched. To obtain a better impedance matching, an extra matching line with length l_t and width w_t is inserted. The operating frequency is assigned as 5.8 GHz, and the conformal array is bent with the bending radius of 20 cm.

2.1. Planar DRA Element

The planar DRA element is firstly designed for an array structure, as shown in Figure 2. The DR element, with the dielectric permittivity of 10, is placed above the ground plane of an F4B substrate ($\epsilon_r = 3.3$, $\tan \delta = 0.003$, $h = 0.5$ mm). The feeding slot is etched on the upper surface of substrate, and the feeding line is placed on the lower surface of the substrate. According to [22], the resonant frequency of rectangle DR antenna element is related to the resonator size and working mode, as Equation (1) listed below:

$$(f_r)_{m,n,p} = \frac{c}{2\pi\sqrt{\epsilon_r}} \sqrt{\left(\frac{m\pi}{l}\right)^2 + \left(\frac{n\pi}{w}\right)^2 + \left(\frac{p\pi}{2h}\right)^2} \quad (1)$$

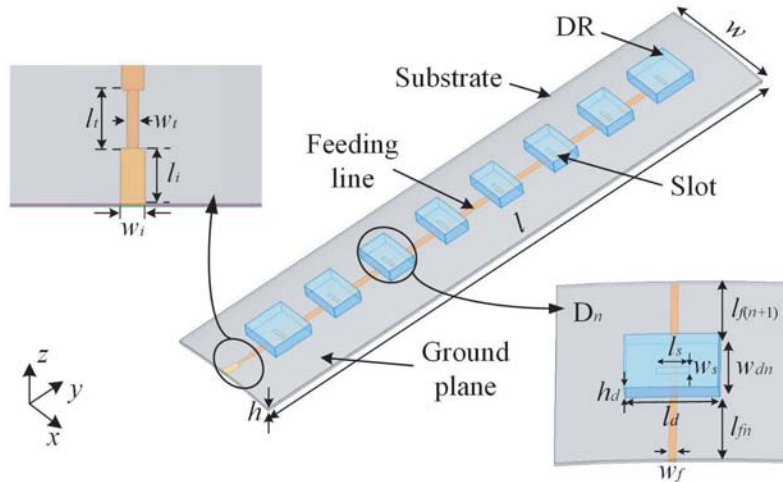


Figure 1. Diagram of the proposed conformal DRA array.

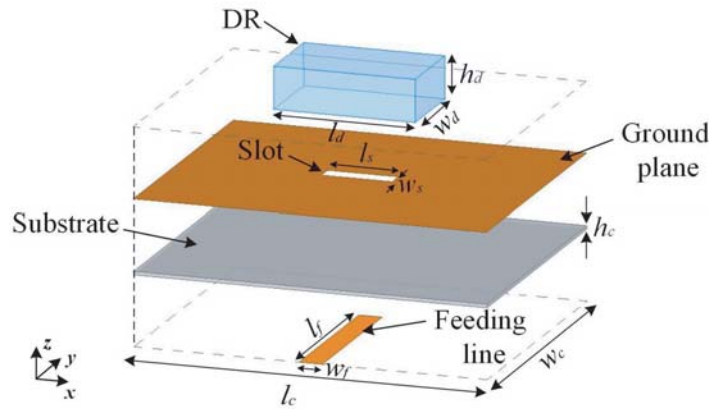


Figure 2. Geometric configuration of the proposed DRA element. (Design parameters: $l_d = 20$, $w_d = 14.5$, $h_d = 6$, $l_c = 50$, $w_c = 40$, $h_c = 0.5$, $l_f = 23.6$, $w_f = 2.6$, $w_s = 1.5$, and $l_s = 7$. Unit: mm.)

Here, f_r represents the resonant frequency of the DR element, c the speed of light in vacuum, and ϵ_r the permittivity of the DR element. Variables m , n , and p represent the numbers of half-waves along the x -, y -, and z -axes, respectively. Variables l , w , and h represent the lengths of the rectangle DR elements along the x -, y -, and z -axes, respectively.

Since two degrees of freedom exist in determining the dimension of the rectangle DR, two conditions are applied in the design including that the length-width ratio (l_d/w_d) of the DR is preset as 1.38 ($l_d > w_d > h_d$) and l_d preset as 20 mm. Besides, assume that the DR element works at the dominant mode of TE_{111}^x ($m = 1$, $n = 1$, and $p = 1$), then the value of h_d can be calculated as 5.7 mm according to Eq. (1). After optimization using the simulation software Ansoft HFSS, the optimized height of the DR element is determined to be 6 mm.

2.2. Conformal DRA Array

A conformal array is firstly constructed based on the eight curved DRA elements with the same dimensions of the proposed DR element. To excite and keep each DRA element in-phase, the intervals between the adjacent slots (d) are assigned as λ_g , where λ_g is the guided wavelength at the working frequency. Since the center frequency is 5.8 GHz, the value of d is calculated as 30.9 mm. Figure 3(a) shows the simulated radiation pattern of the DRA array when $d = 30.9$ mm. It is observed that the radiation beam of the array points to $\theta = -2^\circ$, and a slight shift is exhibited. To optimize the radiation

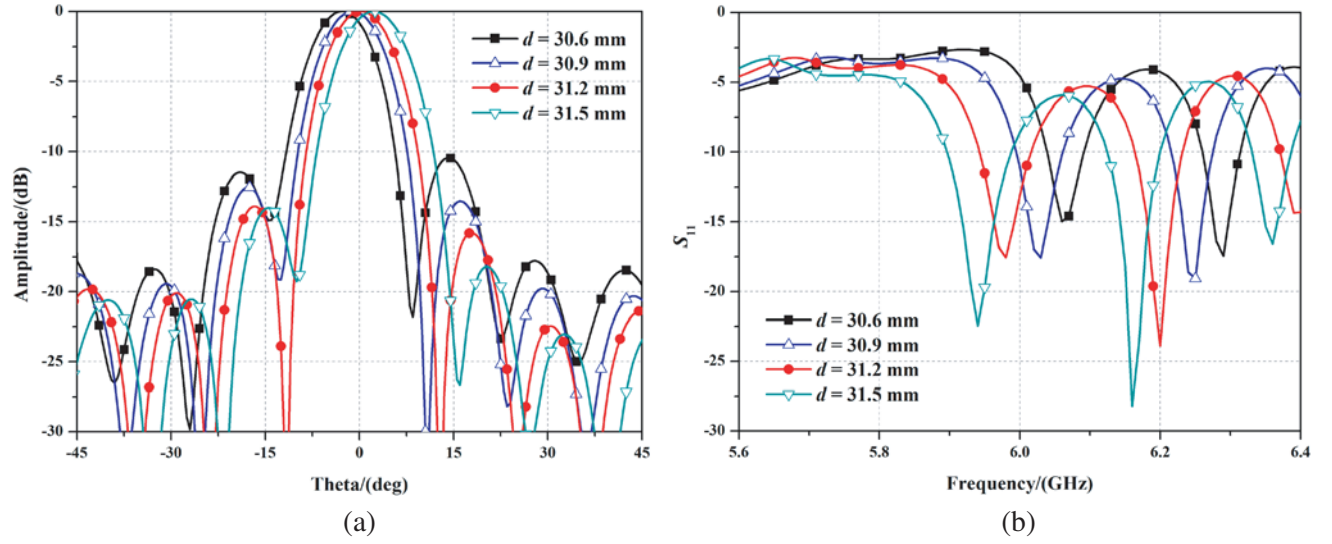


Figure 3. Simulated results of the DRA array under different intervals between the parallel slots. (a) Radiation pattern on yz -plane (E -plane), (b) $|S_{11}|$ results.

performance of the antenna, the DRA array is simulated when d is increased from 30.6 mm to 31.5 mm with the step of 0.3 mm ($0.01\lambda_g$). Figure 3(a) shows the results. It is revealed that when d varies from 30.6 mm to 31.5 mm, the SLL of the radiation pattern is reduced from -10.4 dB to -14.8 dB, and the beam pointing is shifted from -2.5° to 2° . Detailed data are shown in Table 1. The effects of d on the resonate frequency of the DRA array are also investigated, as shown in Figure 3(b). It is found that as d increases from 30.6 mm to 31.5 mm, the resonant frequency of the DRA array is decreased from 6.06 GHz to 5.94 GHz. Since the resonant frequency can be tuned by inserting an extra impedance line, the value of d is finally determined as 31.2 mm after considering to form a beam pointing at $\theta = 0^\circ$.

Table 1. Detailed data in Figure 3 with different values of d .

d (mm)	30.6	30.9	31.2	31.5
Beam pointing ($^\circ$)	-2.5	-2	0	2
SLL (dB)	-10.4	-12.6	-14.8	-14.9
Freq. (GHz)	6.06	6.02	5.98	5.94

2.2.1. Optimization of SLL Performance

In order to improve the anti-interference performance of the DRA array in wireless communication systems, lower SLL is necessary. In this section, the current distributions of the DRA array are shaped to obtain low SLL. In traditional series-fed DRA array, the commonly used methods for controlling the amplitude distribution of the excitation current are feeder width gradation methods, which will increase the complexity of the feeding network. In this design, DRA element width gradation method is firstly applied to shape the current distributions. It has the advantages of smaller size, less complexity, lower attenuation loss, and easy fabrication. Since it is verified that the size of the DR along the feeding line is the main factor that affects the coupling energy between DR elements, the current distribution of the array can be adjusted by the width of the DR. In the design, the widths of DR elements are symmetrically adjusted to obtain tapered current distribution, and low SLL can be obtained. The efficiency of the proposed method can be verified by the optimized simulation results with the aid of simulation software. Table 2 shows the optimized width of the DR elements of the array.

In Figure 4, the E -field distribution of the conformal array with width-gradated elements is

Table 2. Optimized parameters of width-gradated DR elements.

Parameter	w_{d1}	w_{d2}	w_{d3}	w_{d4}	w_{d5}	w_{d6}	w_{d7}	w_{d8}
Value(mm)	20	14.5	13.5	12.5	12.5	13.5	14.5	20

compared with that of the uniform elements. The width-gradated structure makes the energy concentrated at the middle part of array and realizes low SLL characteristic. Although the electric field of the proposed design presents a non-absolutely symmetrical distribution due to the feeding line loss, the SLL and radiation characteristic are similar to those using Chebyshev tapered distribution [23].

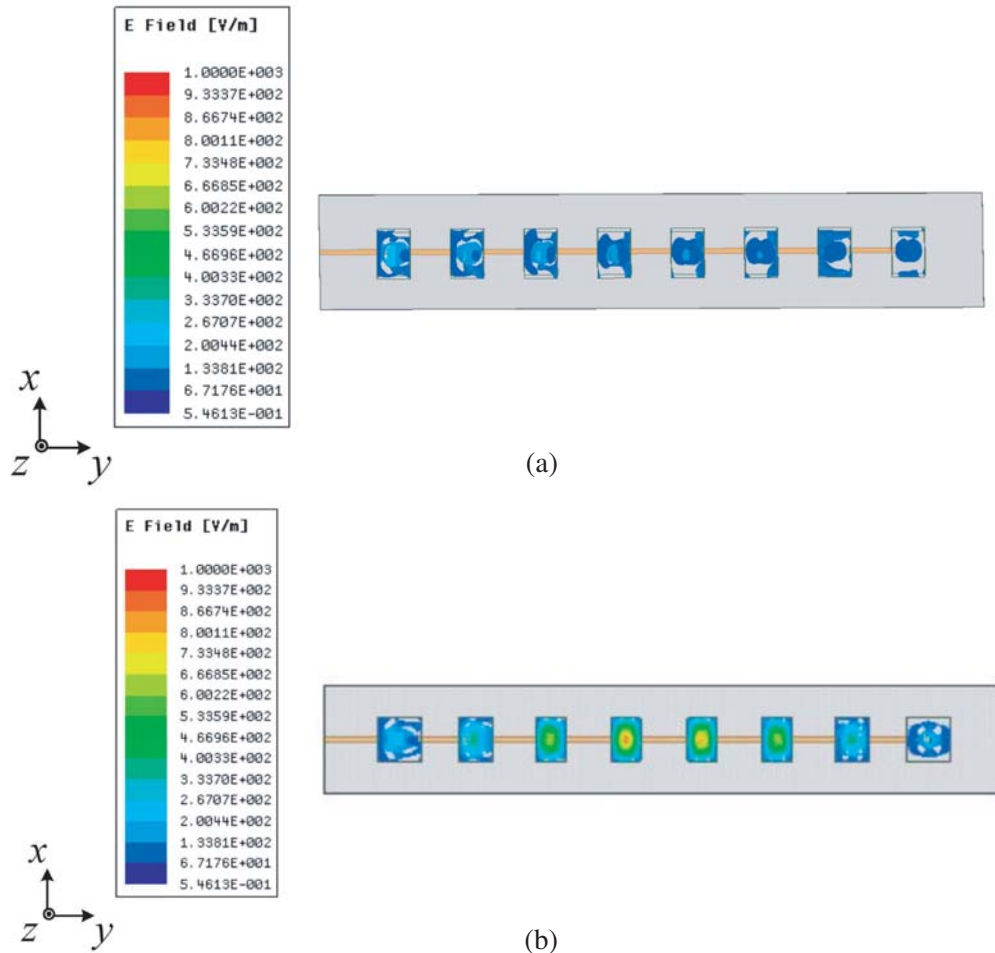


Figure 4. E -field of the proposed array with (a) uniform DRA elements and (b) gradually-widened size DRA elements.

Figure 5 exhibits the effect of the width of the DR elements (w_d) on the directivity and $|S_{11}|$ results of the array at 5.8 GHz. Table 3 shows the detailed data. It is seen that the array with uniform DR elements exhibits the SLL of -13.84 dB. By only optimizing the sizes of the outer and center DR elements symmetrically, the SLL can be reduced to -15.8 dB and -18.4 dB, respectively. It is found that the width of center elements has greater impact on the current distribution of array than the width of outer elements. Further, by tapering the value of w_d from center to the sides symmetrically, the array offers an SLL of less than -21 dB. However, it is revealed from Figure 5(b) that by tuning the width of the DR elements, resonant frequency of the array is slightly shifted. Thus, impedance matching technology should be applied to obtain better impedance characteristic for actual application.

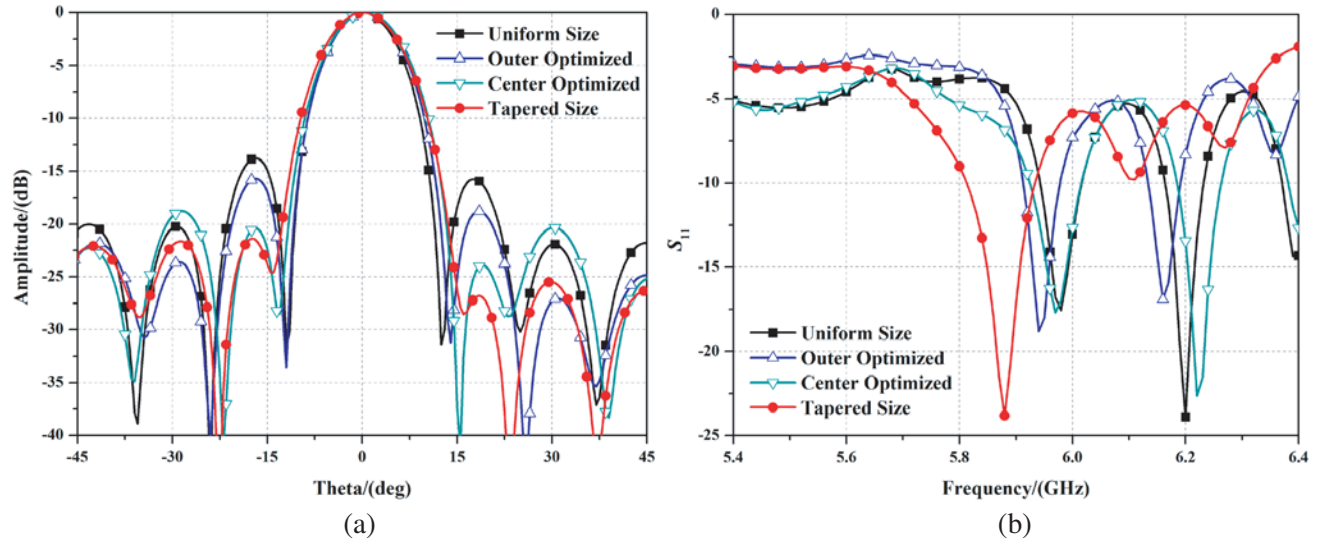


Figure 5. Simulated (a) directivity and (b) $|S_{11}|$ results of the conformal DRA array at 5.8 GHz with different DR width distribution.

Table 3. Detailed data in Figure 5 with different DR width distribution.

DR width distribution	Uniform	Outer Optimized	Center Optimized	Tapered
SLL (dB)	-13.84	-15.8	-18.4	-21.3
Freq. (GHz)	5.99	5.98	5.95	5.88

The advantages of the proposed DRA element width gradation method are as follows. Firstly, since the radiation elements and feeding line are separated by the ground plane, the interference of the feeding line is reduced. Secondly, since the graded-width DRA array could provide a tapered current distribution excited by single feeding line, it offers an easy but efficient way to realize low SLL characteristic with a compact size.

2.2.2. Optimization of Matching Performance

As observed from Figure 5(b), the resonant frequency of the DRA array shifts to higher frequency when combining the eight elements. Although resonant frequency of the antenna array is lowered by using tapered current distribution, it is still higher than 5.8 GHz. To further reduce the frequency and maintain good impedance matching, an extra matching line is inserted into the feeding line, which has no influence on the radiation of the DRA array. Figure 6 compares the simulated $|S_{11}|$ results of the DRA array with different widths (w_t) and lengths (l_t) of the matching line. To avoid interference to the input impedance of the antenna port, the insertion position of the matching line is selected as $l_i = 8$ mm. It is observed that the center frequency can be lowered with the decrease of the width (w_t) and length (l_t) of the matching line, and the change of w_t shows more effects on the impedance matching of the array. Finally, $w_t = 1$ mm and $l_t = 7.9$ mm are selected by optimization (the parameters for red line in Figure 6). To obtain better DRA array performance, the intervals between central adjacent DRA elements of the array have been slightly adjusted, and the final parameters are shown in Table 4.

2.2.3. Effects of the Bending Radius

In this section, the effect of the bending radius (R) of the DRA array is discussed. Figure 7 exhibits the simulated $|S_{11}|$ and radiation performance of series-fed conformal array when it is wrapped around cylinders with radii of 16, 17, 20, and 21 cm. Table 5 shows the detailed data. Firstly, the frequency

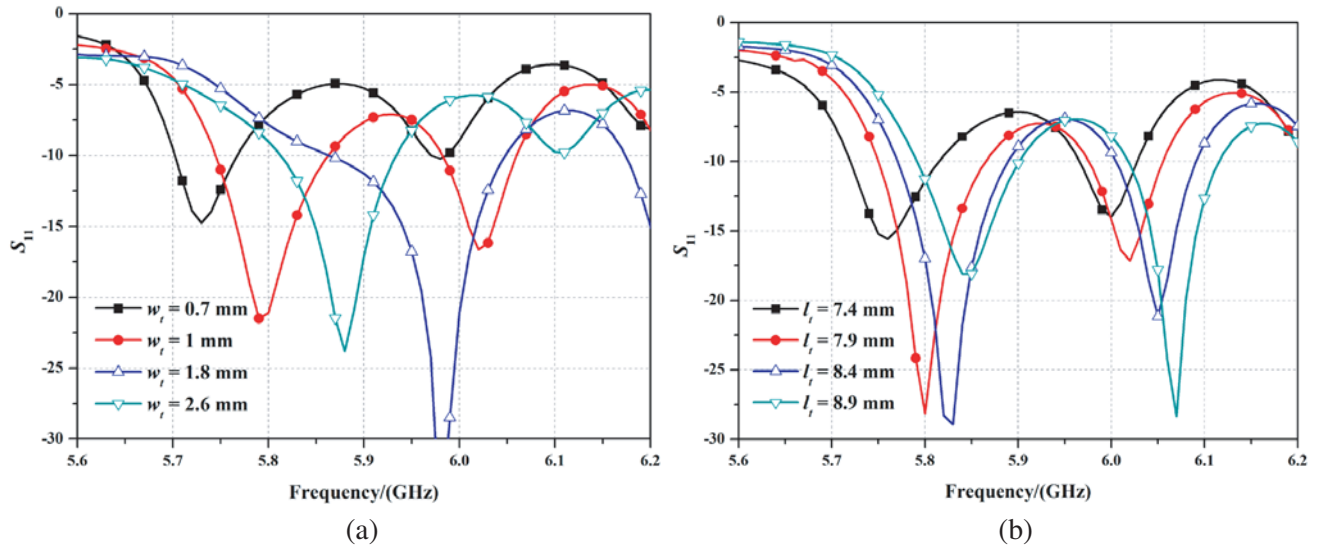


Figure 6. Simulated results of the proposed planar array with different (a) width (w_t) and (b) length (l_t) of impedance matching line, while one parameter is changed, other parameters in Figure 6 are fixed.

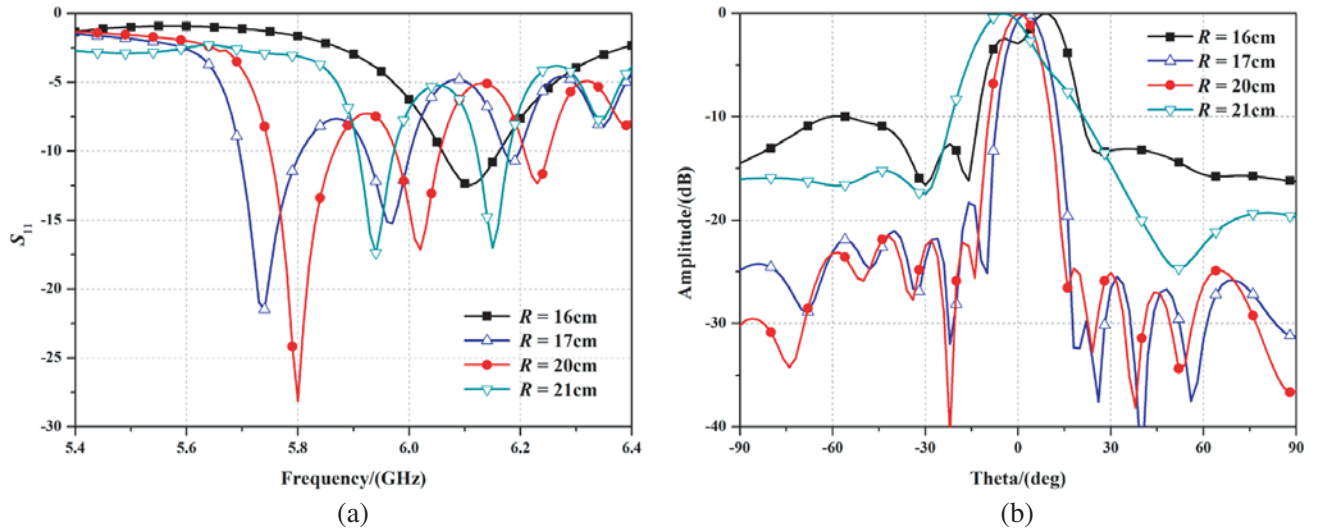


Figure 7. Simulated (a) $|S_{11}|$ and (b) directivity of the conformal DRA array with different bending radius (R).

Table 4. Optimized parameters of the conformal array.

Parameter	w	l	h	w_f	w_t	l_t	l_i	l_d	h_d	w_s
Value (mm)	60	282.1	0.5	2.6	1	7.9	8	20	6	1.5
Parameter	l_s	l_{f1}	l_{f2}	l_{f3}	l_{f4}	l_{f5}	l_{f6}	l_{f7}	l_{f8}	l_{f9}
Value(mm)	7	21.75	13.95	17.2	18.2	18.85	18.2	17.2	13.95	-9.55

shifts to higher frequency when the bending radius R increases from 17 cm to 21 cm. When the radius is changed in the range of 17 cm–20 cm, the changing of bending radius has less effect on the impedance matching of the array. Similarly, when R changes from 20 cm to 17 cm, the beam pointing of the array

Table 5. Detailed data in Figure 7 with different values of R .

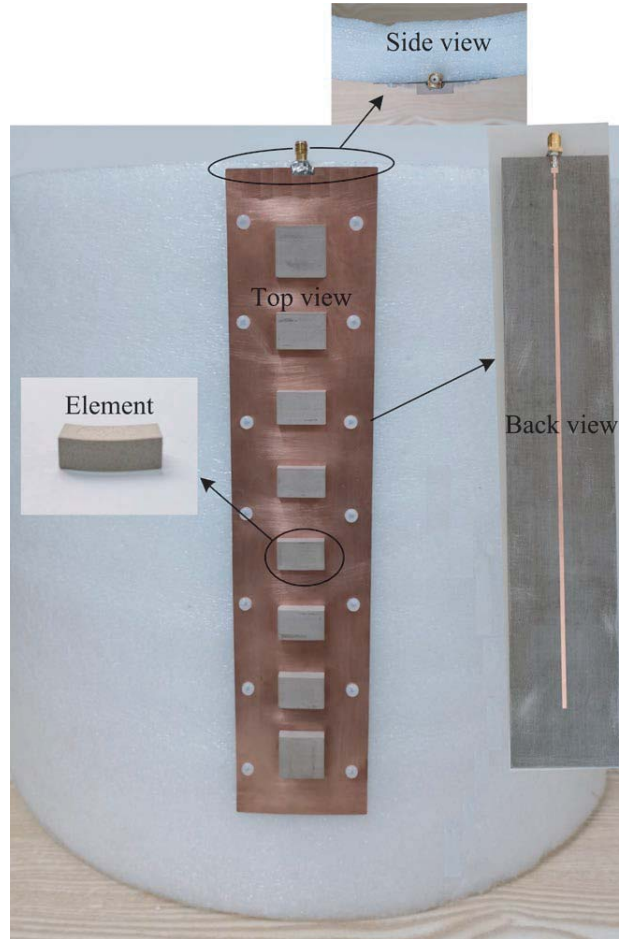
R (cm)	16	17	20	21
Freq. (GHz)	6.1	5.72	5.8	5.95
SLL (dB)	-9.9	-18.6	-21	-15.3
Beam pointing ($^{\circ}$)	10 (split)	2	0	-3

is slightly shifted ($< 2^{\circ}$), and the SLL of the left side is raised by 4.4 dB. However, when R is set as 16 cm or 21 cm, the resonant frequency and the beam pointing is shifted obviously. The SLL is also deteriorated. When R is set as 16 cm, the main beam is split. Thus, a radius error of 3 cm can be tolerated in the fabrication of the supporting cylinder.

3. FABRICATION AND EXPERIMENT RESULTS

The fabricated prototype of aperture-coupled series-fed DRA array is shown in Figure 8. In the fabrication, the DRA array is firstly conformed to a cylindrical support with plastic screws. Then, the curved DR elements are stucked on the ground plane surface of the substrate using glue. The cylindrical support is manufactured using foam material ($\epsilon_r \approx 1$) with an outer diameter of 20 cm.

The fabricated conformal DRA array antennas are measured with the aid of Agilent N5230A and

**Figure 8.** Fabricated prototype of aperture-coupled series-fed DRA array.

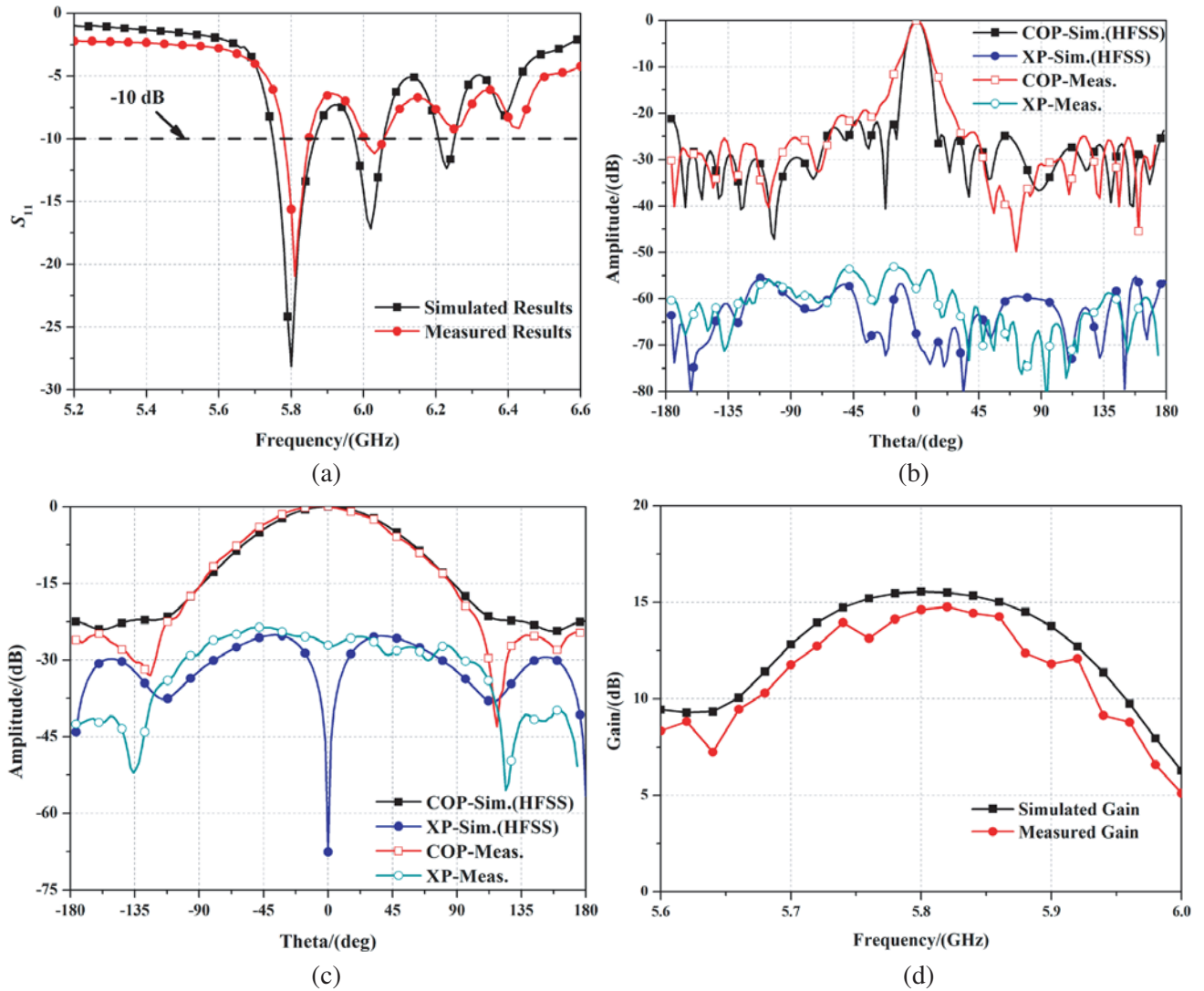


Figure 9. Simulated and measured (a) $|S_{11}|$ results, (b) radiation pattern on yz -plane (E -plane), (c) radiation pattern on xz -plane (H -plane) at 5.8 GHz and (d) gain of the fabricated conformal prototype.

an anechoic chamber. Figure 9(a) shows the simulated and measured $|S_{11}|$ results. It is observed that a good impedance matching of -22 dB is obtained at 5.81 GHz. In the range of 5.78–5.87 GHz, the measured $|S_{11}|$ is less than -10 dB. Figure 9(b) and Figure 9(c) exhibit the radiation patterns of the fabricated prototype on yz -plane (E -plane) and xz -plane (H -plane) at 5.8 GHz, respectively. Obviously, the polarization discriminations between co-polarization (COP) and cross-polarization (XP) of the conformal array are higher than 20 dB in the main radiation direction at the two orthogonal planes. The array offers half-power bandwidth (HPBW) of 10.6° (-4.8° to 5.8°) and 74.5° (-37° to 37.5°) on the E - and H -planes, respectively. The measured results agree with the simulated ones. Besides, a broadside radiation pattern with a measured SLL of -19.3 dB on the E -plane is offered by the antenna array at 5.8 GHz. Figure 9(d) shows that the measured peak gain of the prototype is 14.75 dBi, which is smaller than the simulated result. The difference between the measured and simulated results may be caused by the errors in artificial manufacture process, which is within the tolerance of actual fabrication.

A brief investigation among the proposed and related antenna arrays is tabulated in Table 6. Since no conformal DRA arrays are found, the planar DRA arrays [13, 14, 24] and conformal microstrip

Table 6. Comparison among proposed and related antenna arrays.

Ref.	Type	Element	Freq. (GHz)	Bandwidth* (%)	Gain (dBi)	SLL (dB)	Size ($\lambda_0 \times \lambda_0 \times \lambda_0$)	Conformal
[13]	DRA	8	35	6.3	11.5	-10.5	$8.4 \times 6.4 \times 0.2$	NO
[14]	DRA	8	7.5	38.1	15.7	-23.0	$6.3 \times 1.0 \times 0.3$	NO
[24]	DRA	12	36.5	9	12	NULL	NULL	NO
[25]	Microstrip	7	4.8	3.75	11	-13	$3.7 \times 0.5 \times 0.004$	YES
[26]	Microstrip	8	26	61.5	10.24	-13.49	$6.5 \times 0.8 \times 0.05$	YES
[27]	Microstrip	8	NULL	16.7	14.2	-13.5	$3.84 \times 0.51 \times 0.24$	YES
Prop.	DRA	8	5.8	1.6	14.75	-19.3	$5.5 \times 1.2 \times 0.13$	YES

$$* |S_{11}| < -10 \text{ dB}$$

arrays [25–27] are included. Compared with the DRA arrays in [13] and [24], the proposed structure shows higher gain and lower SLL. Although the array in [14] owns a wider bandwidth and lower SLL, a reflector has to be applied to obtain directional radiation pattern. Besides, since the designs in [13, 14, 24] are planar DRA arrays with large sizes, they are not suitable for the actual application with curved surface. For the conformal arrays, the design in [25–27] offers a compact structure with low profile, but the gains and SLLs are needed to be improved. As indicated, the proposed antenna has the merit of using a compact structure to realize high gain and low SLL, which can be a good candidate for wireless communication systems.

4. CONCLUSION

In this paper, a novel conformal DRA array with high gain, low SLL, and simple structure is presented for wireless communications. The measured results show that the proposed design exhibits $|S_{11}| < -10$ dB over the operating bandwidth from 5.78 GHz to 5.87 GHz. Moreover, a peak gain of 14.75 dBi is obtained at the center frequency with a low SLL of -19.3 dB. The polarization isolation levels of the fabricated prototype in the main radiation direction of E -plane and H -plane are both larger than 20 dB. After comparison among the related literatures, it is illustrated that the proposed design has the advantages of high gain, low SLL, and compact size, which has great potential in the field of 5G micro base stations and wireless communication of smart homes with complex curved surfaces.

ACKNOWLEDGMENT

This work was supported in part by the National Natural Science Foundation of China under Grant 51809030 and Grant 61871417, in part by the Natural Science Foundation of Liaoning Province under Grant 2020-MS-127 and Grant 2019-MS-024, and in part by the Fundamental Research Funds for the Central Universities under Grant 3132020207 and Grant 3132020206.

REFERENCES

1. Mazhar, W., D. Klymyshyn, G. Wells, A. Qureshi, and M. Jacobs, "60 GHz substrate integrated waveguide-fed monolithic grid dielectric resonator antenna arrays," *IEEE Antennas and Wireless Propagation Letters*, Vol. 18, No. 6, 1109–1113, Jun. 2019.
2. Al-Zoubi, A. S., A. A. Kishk, and A. W. Glisson, "Aperture coupled rectangular dielectric resonator antenna array fed by dielectric image guide," *IEEE Transactions on Antennas and Propagation*, Vol. 57, No. 8, 2252–2259, Aug. 2009.
3. Mongia, R. K., "Half-split dielectric resonator placed on metallic plane for antenna applications," *Electronics Letters*, Vol. 25, No. 7, 462–464, Mar. 30, 1989.

4. Luk, K. M. and K. W. Leung, *Dielectric Resonator Antennas*, Research Studies Press, England, U.K., 2003.
5. St. Martin, J. T. H., Y. M. M. Antar, A. A. Kishk, A. Ittipiboon, and M. Cuhaci, "Dielectric resonator antenna using aperture coupling," *Electronics Letters*, Vol. 26, No. 24, 2015–2016, Nov. 1990
6. Kranenburg, R. A. and S. A. Long, "Microstrip transmission line excitation of dielectric resonator antennas," *Electronics Letters*, Vol. 24, No. 18, 1156–1157, Sept. 1, 1988.
7. Gao, Y., Z. Feng, and L. Zhang, "Compact CPW-fed dielectric resonator antenna with dual polarization," *IEEE Antennas and Wireless Propagation Letters*, Vol. 10, 544–547, 2011.
8. Su, M., L. Yuan, and Y. Liu, "A linearly polarized radial-line dielectric resonator antenna array," *IEEE Antennas and Wireless Propagation Letters*, Vol. 16, 788–791, 2017.
9. Althuwayb, A. A., et al., "3-D-printed dielectric resonator antenna arrays based on standing-wave feeding approach," *IEEE Antennas and Wireless Propagation Letters*, Vol. 18, No. 10, 2180–2183, Oct. 2019.
10. Tang, S., X. Wang, W. Yang, and J. Chen, "Wideband low-profile dielectric patch antenna and array with anisotropic property," *IEEE Transactions on Antennas and Propagation*, Vol. 68, No. 5, 4091–4096, May 2020.
11. Shen, W., J. Lin, and K. Yang, "Design of a V-band low sidelobe and wideband linear DRA array," *2016 Progress In Electromagnetic Research Symposium (PIERS)*, 477–480, Shanghai, China, Aug. 8–11, 2016.
12. Abdel-Wahab, W. M., M. Abdallah, J. Anderson, Y. Wang, H. Al-Saedi, and S. Safavi-Naeini, "SIW-integrated parasitic DRA array: Analysis, Design, And Measurement," *IEEE Antennas and Wireless Propagation Letters*, Vol. 18, No. 1, 69–73, Jan. 2019.
13. Abdallah, M. S., Y. Wang, W. M. Abdel-Wahab, and S. Safavi-Naeini, "Design and optimization of SIW center-fed series rectangular dielectric resonator antenna array with 45° linear polarization," *IEEE Transactions on Antennas and Propagation*, Vol. 66, No. 1, 23–31, Jan. 2018.
14. Lin, J., W. Shen, and K. Yang, "A low-sidelobe and wideband series-fed linear dielectric resonator antenna array," *IEEE Antennas and Wireless Propagation Letters*, Vol. 16, 513–516, 2017.
15. Nafea, S. N., "Improving performance of patch antenna for IEEE 802.16e applications using multi-layer antenna structure with reflector," *2018 Al-Mansour International Conference on New Trends in Computing, Communication, and Information Technology (NTCCIT)*, 18–22, Baghdad, Iraq, 2018.
16. Kim, S. and J. Kim, "A circularly polarized high-gain planar 2×2 dipole-array antenna fed by a 4-way gysel power divider for WLAN applications," *IEEE Antennas and Wireless Propagation Letters*, Vol. 18, No. 5, 1051–1055, May 2019.
17. Liu, Y., H. Yang, Z. Jin, F. Zhao, and J. Zhu, "A multibeam cylindrically conformal slot array antenna based on a modified Rotman lens," *IEEE Transactions on Antennas and Propagation*, Vol. 66, No. 7, 3441–3452, Jul. 2018.
18. Zhu, H., X. Liang, S. Ye, R. Jin, and J. Geng, "A cylindrically conformal array with enhanced axial radiation," *IEEE Antennas and Wireless Propagation Letters*, Vol. 15, 1653–1656, 2016.
19. Liu, Y., H. Yang, Z. Jin, and J. Zhu, "Circumferentially conformal slot array antenna and its Ka-band multibeam applications," *IET Microwaves, Antennas & Propagation*, Vol. 12, No. 15, 2307–2312, Dec. 19, 2018.
20. Xiao, S., S. Yang, H. Zhang, Q. Xiao, Y. Chen, and S. Qu, "Practical implementation of wideband and wide-scanning cylindrically conformal phased array," *IEEE Transactions on Antennas and Propagation*, Vol. 67, No. 8, 5729–5733, Aug. 2019.
21. Ogurtsov, S. and S. Koziel, "A conformal circularly polarized series-fed microstrip antenna array design," *IEEE Transactions on Antennas and Propagation*, Vol. 68, No. 2, 873–881, Feb. 2020.
22. Yaduvanshi, R. S. and H. Parthasarathy, *Rectangular Dielectric Resonator Antennas: Theory and Design*, Springer Publishing Company, India, 2016.

23. RanjbarNikkhah, M., J. Rashed-Mohassel, and A. A. Kishk, "A low sidelobe and wideband series-fed dielectric resonator antenna array," *2013 21st Iranian Conference on Electrical Engineering (ICEE)*, 1–3, Mashhad, 2013.
24. Abdel-Wahab, W. M., M. Abdallah, J. Anderson, Y. Wang, H. Al-Saedi, and S. Safavi-Naeini, "SIW-integrated parasitic DRA array: Analysis, design, and measurement," *IEEE Antennas and Wireless Propagation Letters*, Vol. 18, No. 1, 69–73, Jan. 2019.
25. Xu, H., et al., "Wide solid angle beam-switching conical conformal array antenna with high gain for 5G applications," *IEEE Antennas and Wireless Propagation Letters*, Vol. 17, No. 12, 2304–2308, Dec. 2018.
26. Jia, Q., H. Xu, M. F. Xiong, B. Zhang, and J. Duan, "Omnidirectional solid angle beam-switching flexible array antenna in millimeter wave for 5G micro base station applications," *IEEE Access*, Vol. 7, 157027–157036, 2019.
27. Peng, J.-J., S.-W. Qu, M. Xia, and S. Yang, "Wide-scanning conformal phased array antenna for UAV radar based on polyimide film," *IEEE Antennas and Wireless Propagation Letters*, Vol. 19, No. 9, 1581–1585, Sept. 2020.